2009

An investigation of the residual stress characterization and relaxation in peened friction stir welded aluminum–lithium alloy joints

Omar Hatamleh
Iris V. Rivero, *Texas Tech University*
Shayla E. Swain, *Texas Tech University*

Materials and Design 30 (2009) 3367–3373

Contents lists available at ScienceDirect

Materials and Design

journal homepage: www.elsevier.com/locate/matdes

An investigation of the residual stress characterization and relaxation in peened friction stir welded aluminum–lithium alloy joints

Omar Hatamleh [a,*], Iris V. Rivero [b], Shayla E. Swain [b]

[a] Structures Branch, NASA – Johnson Space Center, Houston, TX 77058, United States
[b] Department of Industrial Engineering, Texas Tech University, Lubbock, TX 79409-3061, United States

ARTICLE INFO

Article history:
Received 18 February 2009
Accepted 28 March 2009
Available online 5 April 2009

Keywords:
A. Non-ferrous metals and alloys
C. Surface treatment
E. Fatigue

ABSTRACT

In this investigation the residual stresses generated from friction stir welded (FSW) 2195 aluminum–lithium alloy joints were characterized. The results derived from this research revealed significant levels of tensile residual stresses at the surface and throughout the thickness of the FSW samples. Furthermore, residual stress relaxation at the surface and throughout the thickness of the samples was assessed for laser peened friction stir welded aluminum–lithium joints. To do so the samples were cycled several times at a constant amplitude load. The results indicated that most of the relaxation for the surface residual stresses took place during the first cycle of loading. Also, residual stresses relaxation throughout the thickness of the welded region of unpeened samples significantly exceeded the relaxation exhibited by the laser peened samples.

Published by Elsevier Ltd.

1. Introduction

Aluminum–lithium 2195 alloy is primarily used for aerospace components due to the advantages it presents with respect to fatigue, corrosion resistance, and strength-to-weight characteristics. However, due to the difficulty associated with the welding of this alloy, friction stir welding (FSW) is considered as a candidate process for its welding. Nevertheless, at this point the resultant magnitude and pattern of residual stresses generated by this process requires further understanding. Stresses resulting from applied service loads may not be the only stresses with a direct impact on the fatigue life of structural components. Therefore, the relevance of characterizing the inherent residual stress patterns generated during FSW consists of providing a reference to estimate the fatigue behavior of Aluminum 2195 alloy aerospace components. Mechanical components could be strongly affected by the presence of stresses remaining from processing when deformation forces are unevenly applied and/or in the presence of thermal gradients. In general, residual stresses may arise from a variety of manufacturing processes and techniques. For example, the high temperatures associated with fusion welding lead to the development of complex thermal and mechanical stresses in the weld and its surrounding areas. Following fusion welds, it is common to attain residual stresses approaching the yield strength of the base material. In contrast, FSW takes place at lower temperature levels; thus, resulting in residual stresses which may be considerably less than those observed in fusion welds. At the same time, these residual stresses arising mainly from the thermal cycle and rigid clamping configurations in FSW [1,2], have been shown to affect the fatigue crack growth process [3,4]. Therefore, determination of residual stresses in the FSW joints and surrounding material will play an important role in determining the durability of the welds, and will be fundamental in influencing the welded structural integrity and performance. In doing so, it is very important to have a clear understanding of the residual stress patterns inherited from FSW processing and their effects on structural failure of the components. To accurately predict fatigue crack growth in welded components, it is necessary to understand and track the changes in residual stresses as a function of load cycles. Primarily, since initial residual stresses in welded components may change from their original magnitudes as the specimens are cycled in fatigue testing through either plastic relaxation or cyclic hardening [5].

Laser peening is a surface treatment technique that can introduce higher and deeper compressive residual stresses than those generated by conventional shot peening. The process replaces the stream of particles used in shot peening with short blasts of intense laser light. The laser peening generates high-pressure plasma, which when introduced to metals will create a metallic structure that exhibits significantly improved performance and fatigue life. This peening technique has started to be used in industrial applications including components for aircraft, energy, and naval systems. Therefore, since components whose surfaces have been subjected to laser peening are being fabricated, it is important to understand the residual stress relaxation associated with service of these components. Understanding the pattern of residual stress relaxation of laser peened components will contribute to identifying the role of this process on the components' fatigue life.

* Corresponding author. Tel.: +1 281 483 0286; fax: +1 281 244 5918.
E-mail address: omar.hatamleh-1@nasa.gov (O. Hatamleh).

0261-3069/$ - see front matter Published by Elsevier Ltd.
doi:10.1016/j.matdes.2009.03.038

In this work, the residual stresses generated from friction stir welded 2195 aluminum–lithium alloy joints will be characterized for different size specimens, and the residual stress relaxation as a function of load cycles will be investigated in the specimens. The relaxation study will include several peened and unpeened samples welded from 2195 aluminum alloys (AA). The surface residual stresses will be established using X-ray diffraction (XRD) at several locations across the weld. These locations correspond to the weld nugget, thermo-mechanically affected zone (TMAZ), heat affected zone (HAZ), and base material on both sides of the weld (advancing and retreating). The through thickness residual stresses will also be characterized using the contour method for some FSW samples at 0 and after 1000 cycles of fatigue loading.

2. Experimental procedure

The samples for this investigation were manufactured by FSW of 1.25 cm thick AA 2195 plates. The welding was completed using a probe rotating at a speed of 300 RPM in the counter-clockwise direction, and a translational speed of 15 cm/min. Three different size plates were utilized to assess and characterize the surface and subsurface residual stresses. The dimensions of the plates are shown in Fig. 1. After establishing the residual stresses generated from FSW, a set of specimens with dimensions 41 cm by 10 cm by 1.25 cm were used for the residual stress relaxation portion of the investigation. Some of the specimens were peened using shot peening or laser peening, and some were used in the as-welded condition without any surface processing. Shot peening was performed at an intensity of 0.008–0.012 A. Alternatively, laser peening was performed using a square laser spot with a laser power density of 5 GW/cm^2. The laser was applied three times using a pulse duration of 18 ns. Both surfaces of the specimen were shocked using the same conditions.

XRD was used to measure the surface residual stresses. The measurements were collected at seven different locations across the weld region. These locations corresponded to the weld nugget, TMAZ, HAZ, and base material. In order to establish the magnitude of the surface residual stresses, the lattice strains were assessed through the Multiple Exposure Technique by determining the d-spacings at different ψ directions (where ψ is defined as the angle between the normal to the sample's surface and the normal to the planes from which diffraction occurs). These measurements were then used to derive a plot of $\sin^2\psi$ vs. $\varepsilon_{\phi\psi}$, where "ϕ" is the angle between a reference direction and the direction of stress measurement in the plane, and $\varepsilon_{\phi\psi}$ is the strain in the ϕ and ψ directions. Then from the $\sin^2\psi$ vs. $\varepsilon_{\phi\psi}$ plot, residual stresses were established through the relation defined by Eq. (1) [6]:

$$\sigma_\phi = \frac{mE}{1+\nu} \tag{1}$$

where σ_ϕ = surface stress at a ϕ angle with a principal stress direction; m = slope of the $\sin^2\psi$ vs. $\varepsilon_{\phi\psi}$ plot; ν = Poisson's ratio; E = modulus of elasticity.

Residual stress measurements were collected with a Chromium anode X-ray tube operated at 30 kV and 29 mA. The XRD system detectors were set at a Bragg angle of 157° corresponding to diffraction at the (2 2 2) plane. The maximum β angle was 30° and the number of β angle tilts was set at nine. To reduce the variability, measurements were collected at each location while oscillating the β angle 5° in position. Residual stresses throughout the thickness of the samples were assessed using the contour method and cutting across the welds with an EDM wire. Exposing the cross-sectional plane of the welds allowed the assessment of the residual stresses at different regions across the weld. To minimize thermal deformations that could result from sectioning the samples, the specimens were submerged in water. The parts were also constrained from moving to prevent the cut from deviating from the original cutting plane [7].

Sample cycle loading to investigate residual stress relaxation was performed in a MTS closed-loop universal testing machine. The load was cycled between 0 and 172 MPa upper limit (equivalent to 75% of yield strength) at a stress ratio $R = 0$, starting from low to high. Load cell accuracy is rated at 0.2% of full scale; hence, lower limit was considered effectively zero. The machine was operated in load control mode setting zero as the lower limit to minimize application of any unintended compressive load.

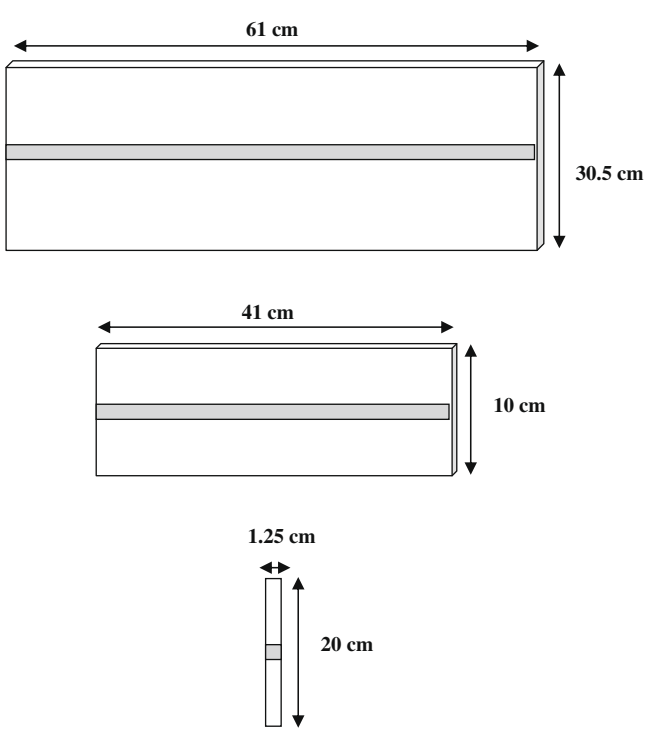

Fig. 1. Geometry of plates used for the residual stress measurements.

3. Results and discussion

The residual stress measurements for the weld nugget in the longitudinal direction for the different plates are shown in Fig. 2. The results indicate that a large amount of surface tensile residual stresses are present after FSW of the large and medium plates. The tensile residual stresses for the large plate had a maximum value of 199 MPa. This location corresponded to the weld interface on the retreating side of the weld. The corresponding value on the advancing side was 189 MPa. The tensile stresses dropped slightly at the weld centerline where the tensile residual stress was 166 MPa. The residual stresses for the medium plate had a similar distribution profile; however, the magnitude of these stresses was reduced. The tensile residual stresses exhibited by the large and medium plates changed to compressive as the distance from the weld centerline increased. This change in residual stress magnitude was the reaction of the material surrounding the weld to balance the tensile residual stresses in the weld region. The surface residual stresses for the small sample plate were mainly in compression at the locations measured.

The residual stresses throughout the thickness of the samples were obtained by means of the contour method and are shown in Figs. 3–5. The magnitude of the measured subsurface residual stresses in the weld for the small sample was relatively small.

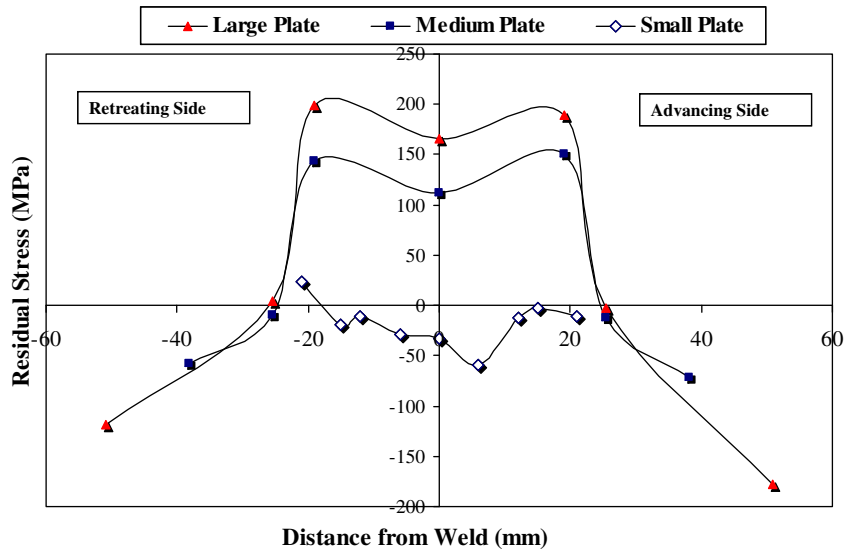

Fig. 2. Longitudinal residual stresses for different plate geometries for FSW 2195.

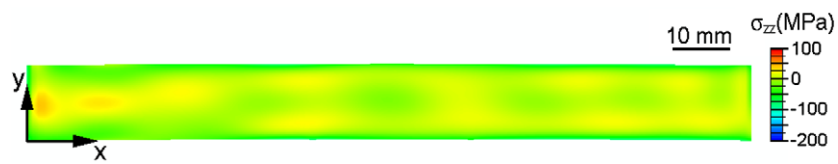

Fig. 3. Two-dimensional map of the measured residual stresses in the unpeened FSW sample for the small 2195 AA specimen.

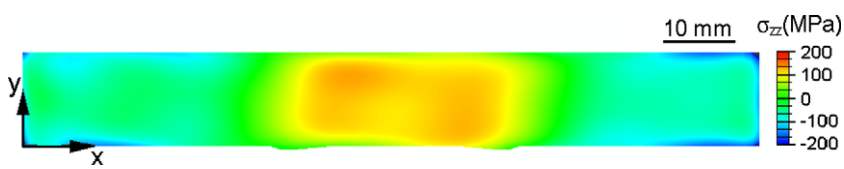

Fig. 4. Two-dimensional map of the measured residual stress for the medium size unpeened FSW specimen.

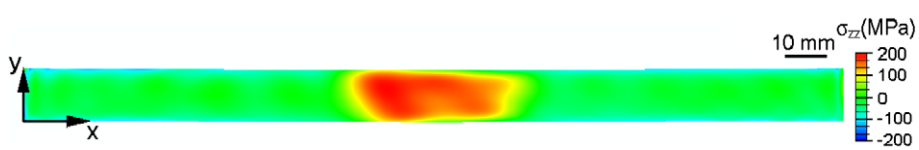

Fig. 5. Two-dimensional map of the measured residual stress for the large size unpeened FSW specimen.

When a small specimen is machined from a large plate, a significant amount of their residual stresses are relaxed and reduced in magnitude. It can be noticed from Figs. 4 and 5 that a significant amount of tensile residual stresses were present in the nugget region, especially through the thickness of the plate. These tensile stresses can be detrimental for the welded components through their service life. Primarily since high tensile residual stresses can result in faster crack initiation, propagation through changes to the effective mean stress during fatigue cycling, and can also reduce mechanical properties. Therefore, special attention is needed when assessing the fatigue life on large welded components by analytical techniques to ensure residual stresses are accounted for in the analysis.

The line plots for the small, medium and large plates are illustrated in Fig. 6. The line plots show a maximum tensile residual stress in the advancing side of the weld around 200 MPa. On the other hand, the correspondent value for the middle sized plate was around 120 MPa. At the end, thorough analysis of these plots confirmed that a behavioral pattern of residual stresses can be discerned in AA 2195 where FSW had been performed. Particularly, it is recognized that the levels of the residual stresses throughout the thickness of the parent material start to get affected approximately 25 mm from the FSW.

The surface residual stresses before and after cycling are illustrated in Figs. 7a–c for the various FSW AA 2195 joints. The figures identify the residual stresses for the as-welded, shot peened, and laser peened samples in the longitudinal direction, respectively. According to the XRD measurements illustrated in Fig. 7a, the tensile residual stress at the center of the plate in the weld nugget for the zero cycle condition was 112 MPa which is approximately 55%

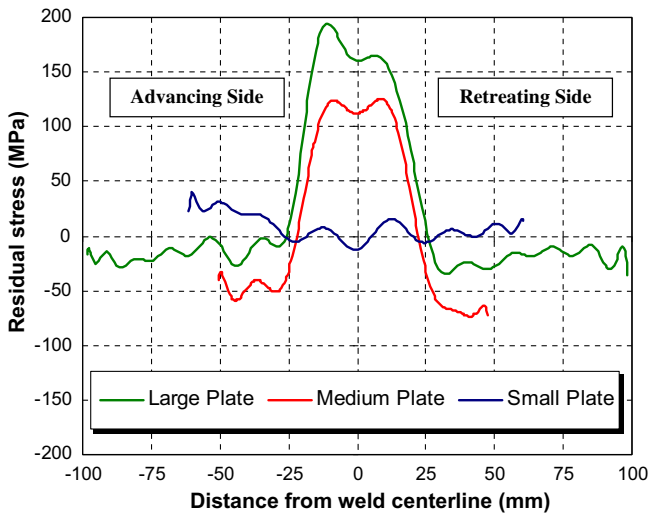

Fig. 6. Line plot of measured residual stress across the width at the approximate mid-thickness of each coupon (y = 6.4 mm).

of the yield stress for that region. The highest tensile residual stress (151 MPa) was collected at the location where the edge of the tool shoulder was near the TMAZ in the advancing side of the weld. The magnitude of residual stresses attained on the advancing side of the weld are associated with the high relative speed developed between the welding tool and the workpiece during processing. High relative speeds during processing lead to the development of higher temperatures during processing in comparison to those attained in the retreating side of the weld. Overall, the surface tensile residual stresses were located in and around the weld, changing to compressive as the distance from the weld centerline increased. The results from this investigation seem to differ from those reported by Staron et al. [8] who indicated that the highest longitudinal tensile stresses were around 130 MPa at a location corresponding to the heat affected zone. The difference in the magnitudes of the residual stresses among the different investigations could be attributed to the different material thicknesses [9], and parameters used during welding (pin diameter, rotation speed and welding speed). These parameters can affect the residual stresses developed during welding.

The results in Fig. 7a also demonstrated that most of the residual stress relaxation in the unpeened FSW samples took place during the first cycle, and minimum change in the magnitude of the residual stresses was identified subsequently. This is consistent with past studies which demonstrated that most of the residual stress relaxation takes place during the first cycle [10,11]. The laser and shot peening process results are shown in Fig. 7b and c revealing significant reduction in the surface residual stresses in the welded joints. The magnitude of the surface compressive residual stresses induced from laser and the shot peening was close in magnitude. All the compressive residual stresses obtained through shot and laser peening remained compressive, even after 1000 cycles. In general, the changes in the residual stresses after the first cycle was highest in the unpeened sample.

The residual stress distributions throughout the thickness of the unpeened or as-welded sample are shown in Fig. 8a at zero cycles and in Fig. 8b at 1000 cycles. The magnitude of the measured subsurface residual stresses in the weld for the unpeened sample in Fig. 8a were relatively high and were mainly concentrated in the weld nugget region. The figure also shows that the highest tensile stresses were not on the surface but on the subsurface of the sample due to increasing constraint. The tensile residual stresses occur as a result of the local frictional heating at the tool–material interface. Specifically, the behavior leading to the tensile residual stresses is associated with hotter material being constrained by variant lower temperature material during cooling [12]. The same sample is also shown in Fig. 8b after 1000 cycles. The results indicate resid-

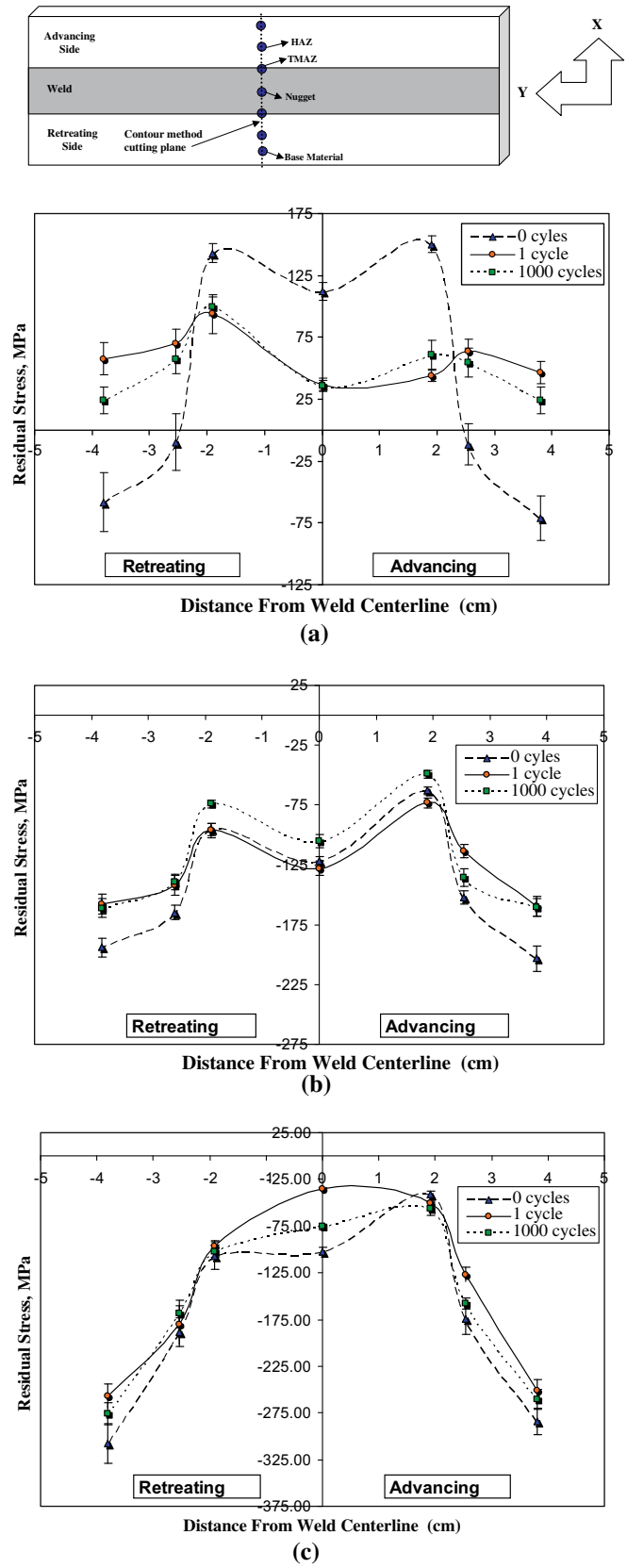

Fig. 7. Longitudinal residual stresses for the FSW 2195 specimens: (a) unpeened, (b) shot peened and (c) laser peened.

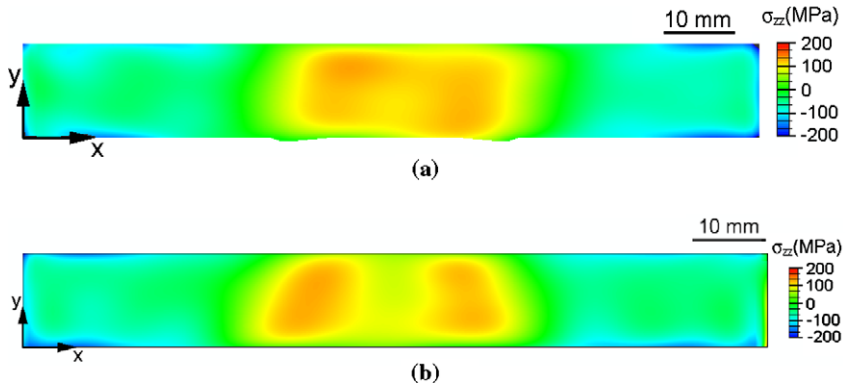

Fig. 8. Two-dimensional map of the measured residual stress for the unpeened 2195 FSW specimen: (a) 0 cycles and (b) 1000 cycles.

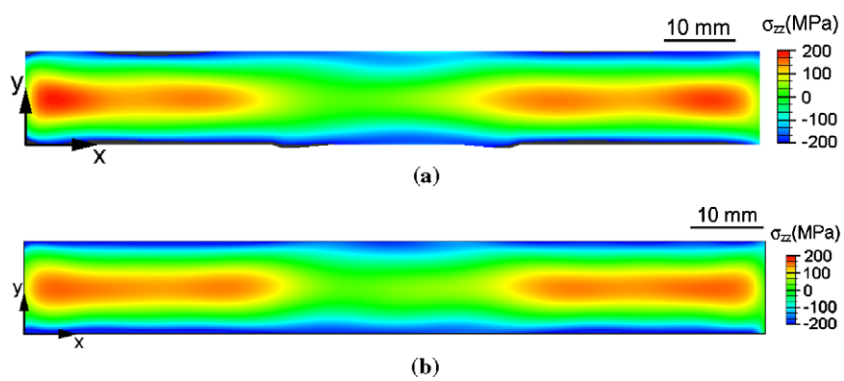

Fig. 9. Two-dimensional map of the measured residual stress for the laser peened 2195 FSW specimen: (a) 0 cycles and (b) 1000 cycles.

ual stress relaxation in the center of the weld nugget following cyclic loading.

Characterization of the laser peened sample shown in Fig. 9a revealed that very significant levels of compressive residual stress were generated near the surface. These results had a drastic effect on the overall residual stress state of the laser peened sample and led to substantial levels of sub-surface compensating tensile residual stresses. It was also noted that the subsurface residual stresses shifted away from the weld region area after peening. The residual stresses for the laser peened sample after cyclic loading shown in Fig. 9b demonstrated an insignificant change in the magnitude of residual stresses throughout the thickness of the sample. King et al. [13] investigated the effects of fatigue loading at $R = 0$ on relaxation for laser peened Ti–6Al–4V under service representative conditions. The study indicated that no significant change to the distribution of the residual stresses was noted. Another investigation by Nalla et al. [14] on laser peened Ti–6Al–4V samples indicated a residual stress relaxation around 20% after fatigue loading at a stress ratio $R = -1$. Since a portion of the loading cycle was performed in compression for the fully reversible cycling condition ($R = -1$), King et al. [13] attributed the relaxation in the $R = -1$ condition to the fact that near surface plastic deformation during the compressive part of the cycle may have been responsible for the relaxation. However, the results in this investigation exhibited different behavior than those reported by King et al. [13] and Nalla et al. [14] since the samples used in this work were fabricated using FSW, and there were already some inherited residual stresses in the samples even before the peening process was introduced.

To compare the results in a quantitative manner, line plots of residual stresses versus depth from the samples' surface were constructed on the center of the weld for both the as-welded and the laser peened specimen (Fig. 10a). These plots demonstrate the effectiveness of laser peening in reducing the tensile residual stresses generated from the welding process. The compressive stresses from laser peening were generated through a depth of 4.0 mm, then changing to tensile due to self-equilibration. Fig. 10a also shows some decrease in the compressive residual stresses after cycling, especially at a depth of 1.5–4 mm from the surface of the processed sample. Nevertheless, high levels of compressive residual stresses persisted up to 3.5 mm from the surface even after being subjected to 1000 cycles of high applied stresses.

Fig. 10b, on the other hand, illustrated the difference in residual stresses through different regions of the weld at the mid-section of the sample. For example, the self equilibrating tensile residual stresses in the center of the sample exhibited minor changes in the overall final attained magnitude of residual stresses. However the unpeened samples indicated a significant drop in the magnitude of the tensile residual stresses at the center of the weld following cyclic loading (about 40 MPa). A previous investigation by Hatamleh [15] indicated that this region of the weld exhibited the weakest tensile properties, and was attributed to the coarsening and/or dissolution of the strengthening precipitates induced by the thermal cycle during the welding process.

The surface residual stresses obtained through the contour method are generally less accurate when compared to those attained through X-ray diffraction; however, comparisons with neutron diffraction measurements show the contour method can accurately measure through thickness residual stresses [16]. Near the surface measurements with contour method present additional noise in the data. The noise may be due to machining irregularities at the edge of the samples or introduced by the coordinate

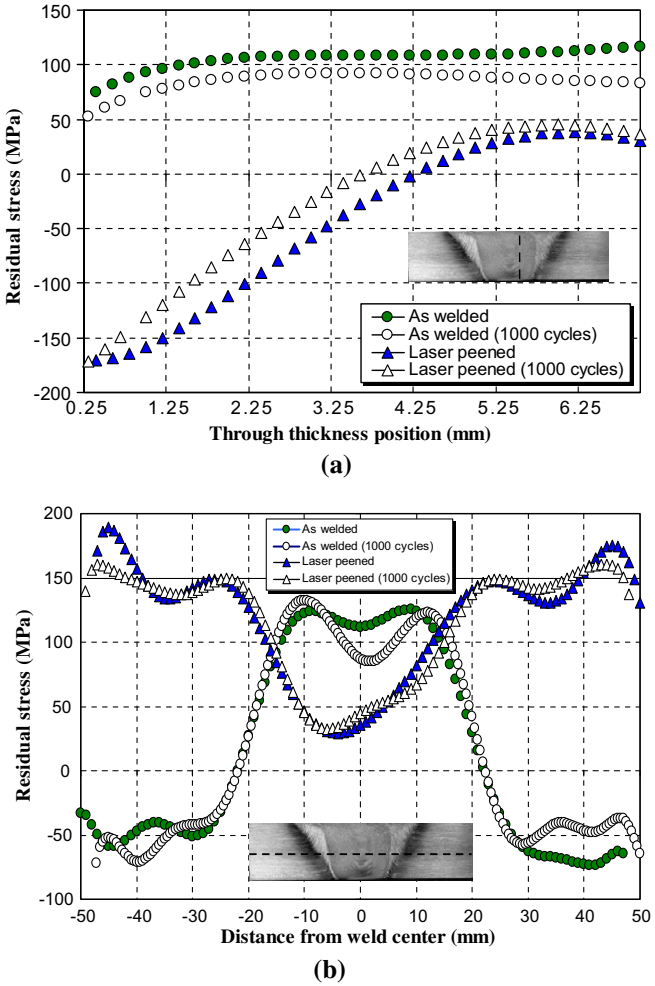

Fig. 10. Line plots of measured residual stress: (a) (through thickness) for the as-welded and the laser peened FSW specimens and (b) distance from the weld center at the approximate mid-thickness of the welds ($y = 6.5$ mm).

measuring machine's spherical tip going slightly past the edge of the part [17]. Therefore, the stress gradient at the surface tends to produce a large displacement gradient which is difficult to distinguish from the noise in the data (surface roughness from cutting and measurement noise). To produce a reasonably smooth stress map, the noise must be filtered by eliminating the variations in the displacements below some prescribed length scale. The net form of the surface is then used to calculate the residual stresses. Consequently, surface residual stresses are better characterized through X-ray diffraction.

4. Conclusions

Overall, this research presents a comprehensive characterization of the residual stresses generated from FSW in 2195 AA. Specifically, the effect of plate size is being analyzed, along with the relaxation of residual stresses as a function of number of cycles. The plate size effects were analyzed revealing that a distinct residual stress pattern occurs for small plates (1.25 cm × 20 cm) compared to the resultant patterns in medium (10 cm × 41 cm) and large (30.5 cm × 61 cm) plates. With respect to residual stresses, the small plates revealed that the parent material characteristics remain unchanged near and at the weld region. Primarily, the magnitude of residual stresses ranged from −10 MPa to −50 MPa in all regions of the small plates with no apparent residual stress distribution pattern. On the other hand, the medium and large plates showed a change in the magnitude of residual stresses from compressive to tensile at around 25 mm from the weld. The maximum level of tensile residual stresses was attained at the weld nugget/TMAZ interface reaching values of 120 MPa and 200 MPa in the medium and large sized plates, respectively. These results are well correlated to the microstructure of FSW. Finally, the high levels of tensile residual stresses generated at the weld nugget suggest that finishing surface treatments should be performed after FSW in order to improve the integrity of the weld.

In addition, the following can be discerned from the current work:

(1) Laser peening was able to introduce a deep layer of compressive residual stresses up to 4 mm from the surface of the FSW AA 2195 joints.
(2) Most of the surface residual stress relaxation in the unpeened FSW sample occurred after the first cycle.
(3) Only minor dissipation of the residual stresses throughout the thickness of the laser peened samples was noticed after cycling the samples to 1000 cycles.
(4) The subsurface residual stresses shifted away from the weld region area after the laser peening process.
(5) The highest amount of relaxation in the unpeened samples took place in the weakest area of the weld (weld nugget).

Acknowledgments

The authors would like to thank James Mulling from the Institute for Maintenance Science and Technology at the Department of Materials Science and Engineering of North Carolina State University for his assistance on performing initial fatigue testing experiments. In addition, the authors appreciate Denis R. Cormier from the Edward P. Fitts Department of Industrial and Systems Engineering at North Carolina State University for his assistance in the fatigue testing.

References

[1] Mishra RS, Ma ZY. Friction stir welding and processing. Mater Sci Eng 2005;R 50:1–78.
[2] Donne CD, Lima E, Wegener J, Pyzalla A, Buslaps T. Investigations on residual stresses in friction stir welds. In: Third international symposium on friction stir welding; 2001.
[3] Pouget G, Reynolds AP. Residual stress and microstructure effects on fatigue crack growth in AA2050 friction stir welds. Int J Fatigue 2008;30:463–72.
[4] John R, Jata K, Sadananda K. Residual stress effects on near-threshold fatigue crack growth in friction stir welds in aerospace alloys. Int J Fatigue 2003;25:939–48.
[5] James MN, Hughes DJ, Hattingh DG, Bradley GR, Mills G, Webster PJ. Synchrotron diffraction measurement of residual stresses in friction stir welded 5383-H321 aluminium butt joints and their modification by fatigue cycling. Fatigue Fract Eng Mater Struct 2004;27:187–202.
[6] Hilley ME, Larson JA, Jatczak CF, Ricklefs RE. Residual stress measurement by X-ray diffraction – SAE J784a. New York: Society of Automotive Engineers Inc.; 1971.
[7] Prime MB, Sebring RJ, Edwards JM, Baumann JA, Lederich RJ. Contour-method determination of parent-part residual stresses using a partially relaxed FSW test specimen. In: Proceedings of the 2004 SEM X international congress and exposition on experimental and applied mechanics; 2004.
[8] Staron P, Kocak M, Williams S, Wescott A. Residual stress in friction stir-welded A1 sheets. Phys B: Condens Matter 2004;350:e491–3.
[9] Fratini L, Zuccarello B. An analysis of though-thickness residual stresses in aluminum FSW butt joints. Int J Mach Tools Manuf 2006;46:611–9.
[10] Kodama S. The behaviour of residual stress during fatigue stress cycles. In: International conference on mechanical behaviour of materials; 1971.
[11] Sakai T, Akita K, Ohya S, Sano Y, Saito T. The effect of static and fatigue loading on residual stress induced by laser peening. J Soc Mater Sci 2008;57: 648–53.
[12] Prime MB, Gnäupel-Herold T, Baumann JA, Lederich RJ, Bowden DM, Sebring RJ. Residual stress measurements in a thick, dissimilar aluminum-alloy friction stir weld. Acta Mater 2006;54:4013–21.

[13] King A, Steuwer A, Woodward C, Withers PJ. Effects of fatigue and fretting on residual stresses introduced by laser shock peening. Mater Sci Eng A 2006;435–436:12–8.
[14] Nalla RK, Altenburger I, Noster U, Liu GY, Scholtes B, Ritchie RO. Mater Sci Eng A 2003;355:216–30.
[15] Hatamleh O. Effects of peening on mechanical properties in friction stir welded 2195 aluminum alloy joints. Mater Sci Eng A 2008;492:168–76.
[16] Prime MB, Hill M, DeWald A, Sebring R, Dave V, Cola M. Residual stress mapping in welds using the contour method. In: Trends in welding research, proceedings of the sixth international conference; 2003.
[17] Prime MB. Cross-sectional mapping of residual stresses by measuring the surface contour after a cut. J Eng Mater Technol 2001;123:162–8.